SYNTHESIS AND CHARACTERISATION OF ORDERED MESOPOROUS ACID CATALYSTS FOR SYNTHESIS OF BIODEGRADABLE SURFACTANTS

Marcelo BOVERI[1], Javier AGÚNDEZ[2], Isabel DÍAZ[3], Joaquín PÉREZ-PARIENTE[4] and Enrique SASTRE[5,*]

Instituto de Catálisis y Petroleoquímica, CSIC, C/Marie Curie, s/n, Cantoblanco, 28049 Madrid, Spain; e-mail: [1] mboveri@icp.csic.es, [2] jagundez@icp.csic.es, [3] idiaz@icp.csic.es, [4] jperez@icp.csic.es, [5] esastre@icp.csic.es

Received July 4, 2003
Accepted July 31, 2003

Solid acid catalysts based on -SO_3H-grafted MCM-41 mesoporous silica were prepared as catalysts for the synthesis of biodegradable surfactants leading reactions. The influence of hydrothermal synthesis time on properties of the mesoporous matrix and catalytic activity and selectivity of the catalysts in the stearic acid–glycerol esterification were studied.

Keywords: Functionalised mesoporous materials; Zeolites; Molecular sieves; Heterogeneous catalysis; Esterification; Fatty acids; Glycerol; Surfactants.

The synthesis of ordered mesoporous materials (OMM), like the M41S family of molecular sieves[1] has opened a new field in catalysis involving large and bulky molecules. Zeolites are well known microporous molecular sieves, which are excellent catalysts widely used in refining and petrochemical processes, which involve molecules with limited sizes and molecular weights. When bulky molecules participate in the process, these microporous catalysts have a limited use. In this sense, the research on the properties and applications of OMM in processes involving high molecular weight compounds has increased notably during the last years[2–4]. Introducing a variety of functional groups (acid, basic, redox, metals, *etc.*) imparts to OMM interesting properties as catalysts in a broad spectrum of reactions[5,6]. Two different procedures for introducing these functional groups into the mesoporous materials have been described: anchoring of synthesized organic compounds containing precursors of reactive groups by reaction with the silanols present on the surface of the calcined or extracted material[7–12] or a one-step synthesis by co-condensation of precursor silanes in aqueous media, by procedures similar to those used to prepare all-inorganic frameworks[13–19].

doi:10.1135/cccc20031914

Following both methods of functionalisation, precursors of sulfonic acid groups such as (sulfanylalkyl)silanes have been described to prepare acid catalysts[20–25]. These materials have been used in the esterification of polyols with fatty acids with the objective to selectively produce the monoesters[24–27], which are valuable products in food, cosmetic and pharmaceutical industries due to their emulsifying properties and biodegradability[28].

A very recent review[29] described in detail the use of acid solid catalysts, zeolites and, mainly, ordered mesoporous materials, in the esterification of glycerol with fatty acids. A detailed study of the different parameters affecting the performance of the catalysts is presented: the hydrophobicity control of the catalyst surface[25,27], the influence of the nature of the organosulfonic functional groups[25,30] and the influence of the mesoporous structure type[31,32] are discussed.

The role of the pore size of the mesoporous channels on the activity and selectivity of the reaction is also mentioned[27], but a systematic study of the influence of such parameter on the performance of the catalysts has not yet been reported. Corma *et al.*[33] demonstrated that it is possible to obtain pure silica MCM-41 materials with different pore sizes by changing the crystallisation time under controlled synthesis conditions.

The aim of this work has been to analyse in detail the influence of the pore size in the catalytic properties of these materials in the esterification of polyols with fatty acids. This paper describes the synthesis of a variety of MCM-41 materials with different pore sizes, their functionalisation with sulfonic acid groups, characterisation of all these materials and the study of the influence of the aforementioned parameter on the catalytic performance in the esterification of glycerol with stearic acid.

EXPERIMENTAL

Synthesis of the Catalysts

Pure silica MCM-41 samples were obtained from the synthesis of gels with molar composition: SiO_2:0.28 TMAOH:0.12 CTABr:26.2 H_2O. The reagents used were: micronized silica (Aerosil® 200), tetramethylammonium hydroxide (TMAOH, Aldrich, 25 wt.% aqueous solution), cetyltrimethylammonium bromide (CTABr, Aldrich) and distilled water. The reagents were used without subsequent purification. The detailed procedure of synthesis to prepare 175 g of gel is the following: 12.72 g of CTABr is mixed with 115.1 g of deionised water in a polypropylene flask (PP), heated at 35 °C and stirred until dissolution (solution A). An amount of 29.7 g of 25 wt.% TMAOH solution is mixed with 1.75 g of Aerosil® in another PP vessel, and gently stirred until the solution becomes clear (solution B). Solution B is then added dropwise to solution A under mild stirring. The resulting solution is stirred for

another 20 min. Then, 15.7 g of Aerosil® is slowly added (in *ca* 40 min) to the flask under mild stirring. The system is left stirring for another hour (pH *ca* 13).

The gels were hydrothermally treated in a 250-ml Teflon-lined stainless steel autoclave at 150 °C and autogeneous pressure for variable periods from 24 to 240 h. The solid products were recovered by filtration, washed with water and dried at 60 °C overnight. Samples were labeled as Sxxx where xxx indicates the time in the oven at 150 °C in hours: S024, S072, S139, S192, S216 and S240. The occluded organic surfactant was removed by heating the samples (3 °C/min) to 540 °C under steady flow of N_2 (100 ml/min) for 1 h, followed by a stream of air (100 ml/min) for 6 h (samples Sxxx-C). Grafting of the materials was carried out as follows: a suspension of the calcined solid in dry toluene (10 ml per g of solid) is allowed to react overnight with an excess of 5 meq MTPS (trimethoxy(3-sulfanylpropyl)silane), Aldrich) per gram of solid at 116 °C under 10 ml/min of dry N_2 (samples Sxxx-SH). In final step, the thiol groups in the materials were oxidised to -SO_3H with H_2O_2 (33% w/v, solid/liquid ratio of 1:20) at room temperature during 24 h, then filtered and washed with ethanol, treated with 0.05 M H_2SO_4 (40 ml per g of solid) for 30 min and finally filtered and washed with water (samples Sxxx-SO_3H).

Characterisation

X-Ray powder diffraction patterns were collected by using CuKα radiation, on a Seifert XRD 3000P diffractometer operating at low angle (1 to 10°). N_2 adsorption/desorption isotherms were carried on an ASAP 2000 Micromeritics apparatus following the BET procedure. Pore diameter distribution was obtained applying the BJH method to the adsorption branch. Thermogravimetric analyses (TGA) were performed on a Perkin Elmer TGA7 from 30 to 800 °C with a heating rate of 20 °C/min in a stream of air. Analysis of the organic material was performed with a Perkin Elmer 2400 CHNS-analyser. Scanning electron micrographs were recorded using a JEOL JM-6400 microscope operating at 40 kV.

Catalytic Tests

The reagents used for catalytic tests were glycerol (Fluka, 99+%), stearic acid (Aldrich, 95+%), and hexadecane (Aldrich, 99+%). The esterification reaction of glycerol with stearic acid was accomplished directly (without solvent), in a stirred four-neck flask under atmospheric pressure. A N_2 steady flow at 10 ml/min was passed over the reaction mixture through one flask neck in order to remove the water formed during the esterification, which was adsorbed in a glass tube packed with zeolite A. The reaction temperature was measured with a thermometer immersed in the mixture. The reaction temperature range studied was 120–135 °C. A molar ratio fatty acid/glycerol of 1 was set and the amount of catalyst employed – previously dried at 100 °C overnight – was 5.0 wt.%. Hexadecane (10 wt.% in the reaction mixture) was used as internal standard for all tests. The reaction mixture was sampled in regular time intervals ranging between 1 and 24 h.

Reactants and products were analysed by HPLC with an isocratic pump (Waters 1515) connected to a Symmetry® C_{18} 5 μm, 4.6 × 150 mm column and a refractive index detector (Waters 2414). Separation of products was achieved with a 4:4:2 (by volume) acetonitrile/acetone/ dichloromethane mixture as mobile phase, at a flow rate of 1 ml/min. The temperature of the column and the detector was kept constant at 35 °C. Calibration analyses were obtained with pure-grade acid, monoglyceride, diglyceride and triglyceride.

RESULTS AND DISCUSSION

X-Ray diffraction patterns of the as-synthesised samples are presented in Fig. 1. The characteristic profile of the hexagonal symmetry of MCM-41 type structure (p6mm) is observed for all the samples. The sharp and intense peak at a low angle, corresponding to 100 reflection, is accompanied by three weaker reflections (at 2θ close to 3.6, 4.1 and 5.4° for sample S024); corresponding to 110, 200 and 210 reflections, respectively; indicating highly ordered arrangement of pores. At the same time, a shift of the peaks towards lower 2θ values can be clearly observed when the synthesis time increases, up to 192 h. No further shifting was observed beyond the 192 h threshold through the upper limit tested, 240 h. The lower 2θ values correspond to an increase of the interplanar spacing and, consequently, of the unit cell size. Unit cell size values ($a_0 = 2d_{100}\sqrt{3}$) and their evolution with synthesis time are shown in Fig. 2. It becomes evident a linear correlation between a_0 and the hydrothermal synthesis time from 24 to 192 h. Longer crystallisation times do not increase the unit cell size, in good agreement with the observations previously described in the literature[33]. Calcined samples show a contraction of the unit cell of ≈2–3 Å in all the cases[33,34]. The resulting a_0 values follow the same trend with the synthesis time as the as-made samples. This shrinkage could be explained by structure relaxation, which comprises rearrangement of tension-relieving Si–O–Si bonds as well as internal Si–OH condensation, during the thermal treatment. After functionalisation (-SH) and oxidation (-SO_3H), the highly

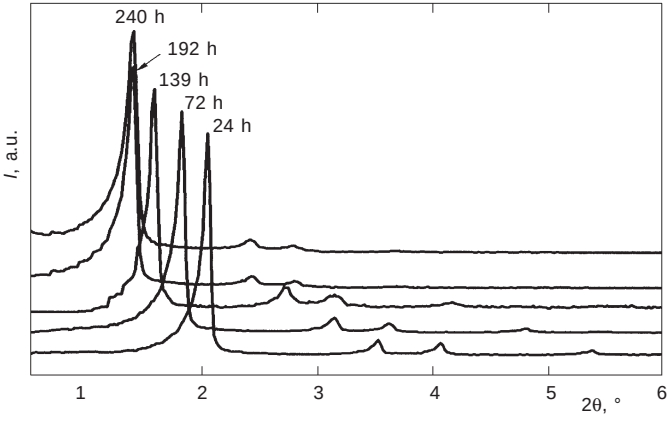

FIG. 1
X-Ray diffraction patterns of as-made samples prepared at increasing crystallisation times

ordered hexagonal structure is maintained, as it is observed in the X-ray diffraction patterns of sample synthesised for 24 h (Fig. 3); and only negligible differences in unit cell parameter can be observed.

Nitrogen isotherm plots of the calcined samples are shown in Fig. 4, shifted on the vertical axis for sake of clarity. Their shapes are characteristic of mesoporous materials. It can be seen that the increase in reaction time results in a shift of the capillary condensation P/P_0 region towards higher

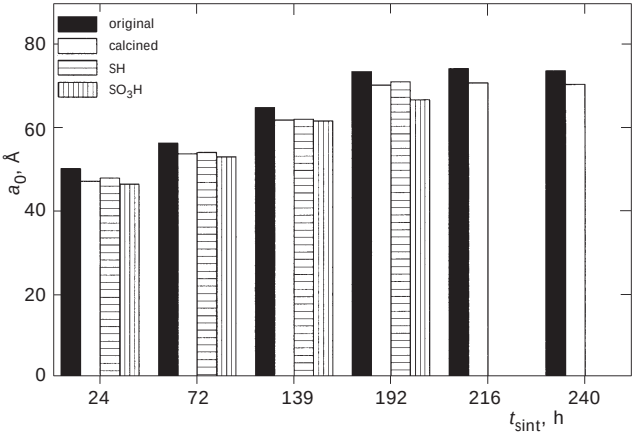

FIG. 2
Unit cell parameter (a_0) of the different samples, as-synthesised, calcined, thiol-functionalised and oxidised

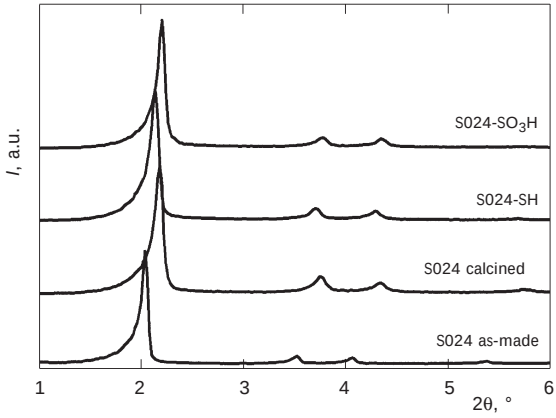

FIG. 3
X-Ray diffraction patterns of as-synthesised S024 material and samples S024 after the different treatments (calcination, functionalisation and oxidation)

relative pressures, which means that the pore size increases with the hydrothermal treatment at 150 °C. This increase correlates with the increase in the a_0 values measured by XRD. A hysteresis loop in the aforementioned zone in samples synthesised for ≥72 h, typical of mesoporous solids with pore diameter larger than 30 Å, is also observed. The scanning electron micrographs shown in Fig. 5 present the evolution of the crystal size and

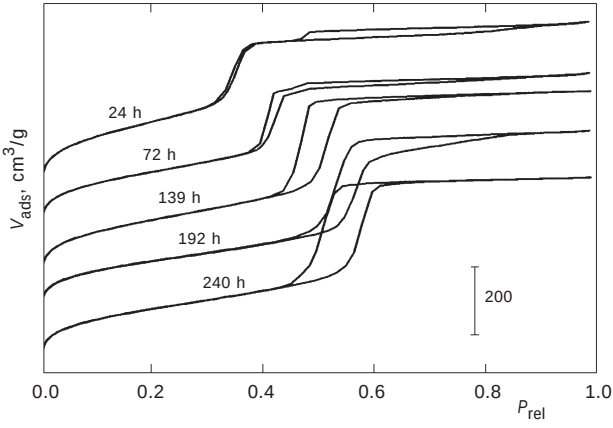

FIG. 4
N_2 adsorption–desorption isotherms of calcined samples synthesised at different crystallisation times

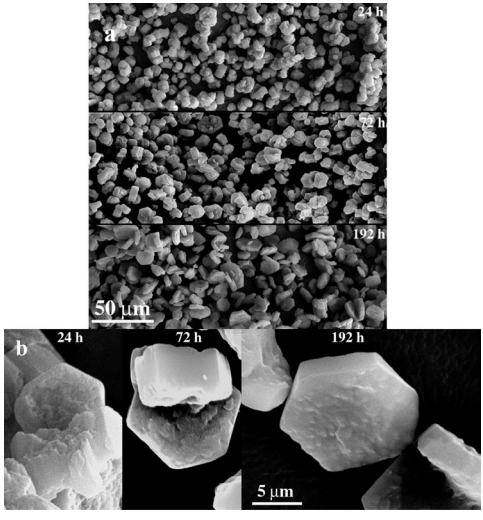

FIG. 5
Scanning electron micrographs of selected as-synthesised samples

shape with the reaction time. It can be observed that all the samples show a homogeneous distribution of crystal size (Fig. 5a). The average size increases with the crystallisation time from ≈7 (sample S024) to ≈13 μm (sample S192) and the crystals in the samples with longer crystallisation times are clearly identified as hexagonal prisms, while the samples obtained at shorter times are poorly defined (Fig. 5b). Sample S072 presents intermediate properties between S024 and S192.

The sharp step in the adsorption isotherms evidences narrow pore size distributions (obtained by the BJH method), centred at larger pore diameter for samples prepared at increasing crystallisation times (Fig. 6). As it was observed in the isotherm plots and in the XRD patterns, samples obtained at crystallisation times above 192 h present similar properties. At the same time, it is worth mentioning that the wall thickness, parameter closely related with the stability of these materials, remains virtually unchanged for all the calcined samples through whole range of reaction times tested, presenting values between 22 and 25 Å (difference between a_0 and d_p).

Table I presents the textural properties calculated from the N_2 adsorption data for different samples. After SH grafting, a decrease in the surface BET area, pore volume and free pore diameter was observed for all the samples, as shown in Fig. 7. This variation can be attributed to the effect produced by the functional SH groups protruding from the pore walls. In fact, thermogravimetric and elemental analyses show the extent of the anchoring of organic compounds in these materials (Tables II and III, Fig. 8).

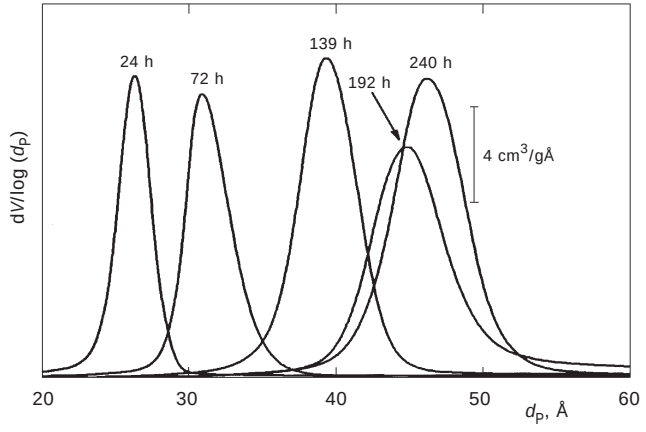

FIG. 6
Pore size distribution (BJH method, adsorption branch) of calcined samples synthesised at different crystallisation times

Figure 8 presents the thermogravimetric analyses of samples S192. All the samples present first a weight loss (T < 200 °C) attributed to adsorbed water. The weight losses observed at T > 200 °C change for the different samples. The as-made sample S192 shows a large weight loss (≈50 wt.%) centred at ≈300 °C, corresponding to the elimination of the surfactant. After calcination, sample S192-C exhibits, in addition to the adsorbed water weight loss (<200 °C), a slight and continuous weight loss through the whole temperature range, which can be attributed to the surface dehydroxylation. Sample S192-SH, functionalised with MPTS, shows a weight loss at ≈350 °C, attrib-

TABLE I
Textural properties of the different samples

Sample	Calcined		-SH		-SO_3H	
	S_{BET}, m^2/g	V_p, cm^3/g	S_{BET}, m^2/g	V_p, cm^3/g	S_{BET}, m^2/g	V_p, cm^3/g
S024	1027	0.93	968	0.75	952	0.75
S072	949	0.96	843	0.78	841	0.78
S139	883	1.01	810	0.88	811	0.88
S192	738	0.99	698	0.86	705	0.86

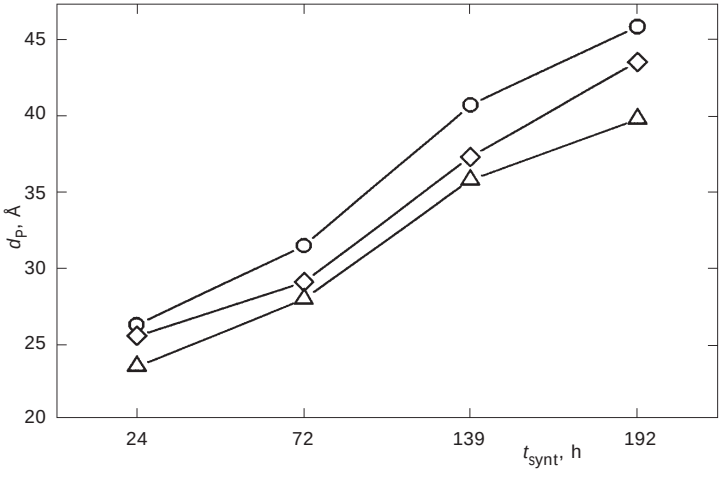

FIG. 7
Changes of the average pore diameter (d_p) of samples synthesised at different crystallisation times: calcined samples (○); -SH samples (△) and -SO_3H samples (◇)

uted to the decomposition of the sulfanylpropyl groups[35]. After oxidation, the propanesulfonic groups are eliminated at higher temperature (≈500 °C), which indicates the higher thermal stability of these groups compared with

TABLE II
Weight losses (in wt.%) calculated from the thermogravimetric analyses of thiol and sulfonic samples

Sample	T < 200 °C			200 °C < T < 800 °C		
	calcined	-SH	-SO_3H	calcined	-SH	-SO_3H
S024	4.2	4.0	10.8	2.9	7.4	7.6
S072	5.2	3.5	7.2	2.4	8.1	8.6
S139	4.6	3.8	8.6	2.7	5.7	6.0
S192	3.3	3.1	7.2	3.1	7.1	6.6

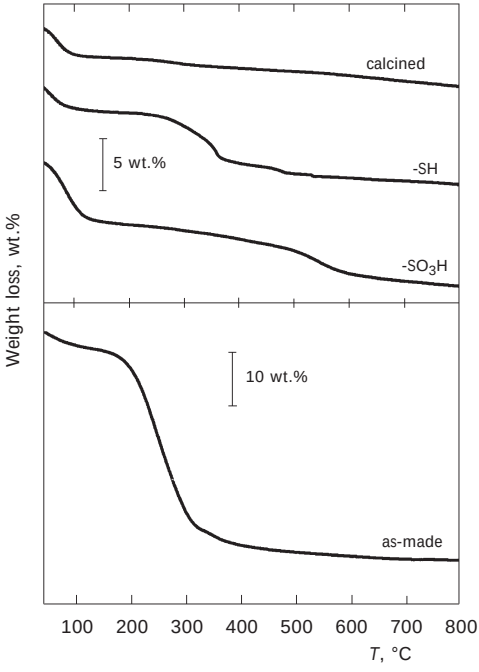

FIG. 8
Thermogravimetric analyses of as-made S192 material and samples S192- after the different treatments (calcination, functionalisation and oxidation)

their thiol precursors, and suggests potential use of these materials in reactions carried out at moderate temperatures. The weight losses for the different samples are detailed in Table II. From the weight losses at <200 °C, attributed to adsorbed water, the higher hydrophilic character of the sulfonic samples can be confirmed. At temperatures above 200 °C, the weight losses observed are practically the same before and after oxidation, which suggests that not all the thiol precursors survive the oxidation stage, due to the higher molecular weight of the -SO_3H group compared with -SH.

The catalytic performance of the sulfonic-MCM-41 materials was tested in the esterification of glycerol with stearic acid at two temperatures and the results were compared with those of a SO_3H-MCM-41 catalyst synthesised by co-condensation, (the synthesis was reported previously), labelled PM0H [27]. Table IV and Fig. 9 summarise some of the results obtained. At 135 °C, an acid conversion above 90% was obtained after 10 h of the reaction for all the catalysts, except S139-SO_3H (Fig. 9). At early stages of the reaction, some differences between the catalysts can be observed. It has been described previously in the literature that there are several factors, which can affect to the activity and selectivity of this reaction, such as the hydrophobic character of the catalysts or the number and nature of the acid centres[29]. In this case, we have tried to minimise these factors in order to compare exclusively the influence of the pore size of the catalysts on the activity and selectivity of the reaction. Data of the thermogravimetric analyses suggest that only minor differences in the hydrophilic/hydrophobic character exist among all the catalysts – sulfonic form of the materials (Table II). However, due to the different number of active centres (related to

TABLE III
Sulfur content of thiol and sulfonic acid samples determined by elemental analyses

Sample	$S_{E.A.}$ [a]	
	-SH	-SO_3H
S024	0.48	0.19
S072	0.39	0.18
S139	0.20	0.08
S192	0.40	0.14

[a] Sulfur determined by elemental analysis (meq/g SiO_2).

the sulfur content in the sulfonic acid samples, Table IV), the activity should be compared on the basis of their turnover numbers (TON), as given in Table IV. The TON values are very similar for the Sxxx catalysts and appreciably higher than those of the reference sample PM0H. As can be observed in Table IV, the amount of sulfur in the co-condensed sample is much higher, but its intrinsic activity is lower, probably due to narrower

TABLE IV
Intrinsic activity and selectivity of the catalysts in the esterfication of glycerol with stearic acid at 120 and 135 °C (acid/glycerol molar ratio 1:1; catalyst: 5 wt.%)

Sample	*S* content meq/g_{cat}	d_p, Å	120 °C		135 °C	
			TON[a]	selectivity[b]	TON[a]	selectivity[b]
S024-SO_3H	0.16	26	13.0	61	48.0	54
S072-SO_3H	0.16	29	–	–	36.6	48
S139-SO_3H	0.07	37	–	–	40.5	51
S192-SO_3H	0.12	44	13.0	59	56.1	59
PM0H	0.97	21	4.4	68	10.3	64

[a] Turnover ($mmol_{ac}/meq_S$ h) calculated at 6 h. [b] Selectivity (%) to monostearate at 50% acid conversion. [c] Turnover ($mmol_{ac}/meq_S$ h) calculated at 8 h.

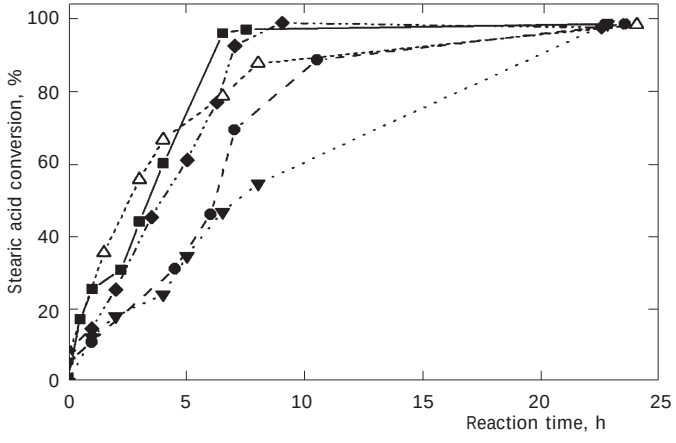

FIG. 9
Stearic conversion *vs* reaction time for the different catalysts: S024-SO_3H (■), S072-SO_3H (●), S139-SO_3H (▼), S192-SO_3H (◆), PM0H (△)

pore diameters of this sample. In a previous paper it has been described that the intrinsic activity of this kind of catalysts in the esterification of fatty acids with glycerol changes appreciably when the acid chain length varies[24,27], and small changes in the pore size of the material can drastically affect the activity and selectivity of the catalysts. The selectivity values (obtained at an acid conversion of 50 %) are also presented in this Table. It can be observed that the more active catalysts (S024-SO_3H, S192-SO_3H and PM0H) show a higher selectivity to the monoglyceride at 135 °C, while the two catalysts less active, S072-SO_3H and S139-SO_3H, show lower selectivity to the monostearate. This can be due to the relative contribution of the non-selective homogeneous reaction to the global activity, which becomes more important at higher temperatures[24]. In addition, a slightly higher selectivity of the co-condensed catalysts can be observed at both reaction temperatures. The reason for that can be attributed to lower pore diameters of this catalyst, which, in addition to inhibiting the reaction inside the pores as was suggested, makes more difficult the formation of the bulky secondary products, di- and triglycerides, inside the pores, which leads to an increase in the selectivity to monoglyceride.

This work has been supported by the Comunidad Autónoma de Madrid (Spain) CAM: Project 07M/0048/2002. M. Boveri thanks MECD (Spain) for the Ph.D. grant.

REFERENCES

1. Beck J. S., Chu C. T. W., Johnson I. D., Kresge C. T., Leonowicz M. E., Roth W. J., Vartuli J. W.: WO Pat. 91/11390 (1991).
2. Corma A.: *Chem. Rev. (Washington, C. D.)* **1997**, *97*, 2373.
3. Biz S., Ocelli M. L.: *Catal. Rev.-Sci. Eng.* **1998**, *40(3)*, 329.
4. Davis M. E.: *Nature* **2002**, *417*, 813.
5. Stein A., Melde B. J., Schroden R. C.: *Adv. Mater.* **2000**, *12*, 1403.
6. Sayari A., Hamoudi S.: *Chem. Mater.* **2001**, *13*, 3151.
7. Feng X., Fryxell G. E., Wang L. Q., Kim A. Y., Liu J., Kemmer K. M.: *Science* **1997**, *276*, 923.
8. Liu J., Feng X., Fryxell G. E., Wang L. Q., Kim A. Y., Gong M.: *Adv. Mater.* **1998**, *10*, 161.
9. Lim M. H., Blanford C. F., Stein A.: *J. Am. Chem. Soc.* **1997**, *119*, 4090.
10. Lim M. H., Blanford C. F., Stein A.: *Chem. Mater.* **1998**, *10*, 467.
11. Antochshuk V., Jaroniec M.: *Chem. Commun.* **1999**, 2373.
12. de Juan F., Ruiz-Hitzky E.: *Adv. Mater.* **2000**, *12*, 430.
13. Macquarrie D. J.: *Chem. Commun.* **1996**, 1961.
14. Macquarrie D. J., Jackson D. B., Mdoe J. E. G., Clark J. H.: *New. J. Chem.* **1999**, *23*, 539.
15. Fowler C. E., Burkett S. L., Mann S.: *Chem. Commun.* **1997**, 1769.
16. Lebeau B., Fowler C. E., Hall S. R., Mann S.: *J. Mater. Chem.* **1999**, *9*, 2279.

17. Mercier L., Pinnavaia T. J.: *Chem. Mater.* **2000**, *12*, 188.
18. Corriu R. J. P., Hoarau C., Mehdi A., Reye C.: *Chem. Commun.* **2000**, 71.
19. Marlogese D., Melero J. A., Christiensen S. C., Chmelka B. F., Stucky G. D.: *Chem. Mater.* **2000**, *8*, 2448.
20. Lim M. H., Blanford C. F., Stein A.: *Chem. Mater.* **1998**, *10*, 467.
21. Van Rhijn W. M., De Vos D. E., Bossaert W., Bullen J., Wouters B., Grobet P. J., Jacobs P. A.: *Stud. Surf. Sci. Catal.* **1998**, *117*, 183.
22. Van Rhijn W. M., De Vos D. E., Bossaert W., Jacobs P. A.: *Chem. Commun.* **1998**, 317.
23. Díaz I., Márquez-Alvarez C., Mohino F., Pérez-Pariente J., Sastre E.: *J. Catal.* **2000**, *193*, 283.
24. Díaz I., Mohino F., Pérez-Pariente J., Sastre E.: *Appl. Catal., A* **2001**, *205*, 19.
25. Díaz I., Mohino F., Pérez-Pariente J., Sastre E.: *Appl. Catal., A* **2003**, *242*, 161.
26. Bossaert W. D., De Voos D. E., Van Rhijn W. M., Bullen J., Wouters B., Grobet P. J., Jacobs P. A.: *J. Catal.* **1999**, *182*, 156.
27. Díaz I., Márquez-Alvarez C., Mohino F., Pérez-Pariente J., Sastre E.: *J. Catal.* **2000**, *193*, 295.
28. Henry C.: *Cereal Foods World* **1995**, *40*, 734.
29. Pérez-Pariente J., Díaz I., Mohino F., Sastre E.: *Appl. Catal., A* **2003**, in press.
30. Mohino F., Díaz I., Pérez-Pariente J., Sastre E.: *Stud. Surf. Sci. Catal.* **2002**, *142*, 1275.
31. Díaz I., Pérez-Pariente J., Sastre E., Wright P. A., Zhou W.: *Stud. Surf. Sci. Catal.* **2001**, *135*, 1248.
32. Díaz I., Mohino F., Sastre E., Pérez-Pariente J.: *Stud. Surf. Sci. Catal.* **2001**, *135*, 1383.
33. Corma A., Kan Q., Navarro M., Pérez-Pariente J., Rey F.: *Chem. Mater.* **1997**, *9*, 2123.
34. Ortlam A., Rathousky J., Schulz-Ekloff G., Zukal A.: *Microporous Mater.* **1996**, *6*, 171.
35. Díaz I., Mohino F., Pérez-Pariente J., Sastre E.: *Thermochim. Acta* **2003**, in press.